Tests of gravitational-wave birefringence with the open gravitational-wave catalog

Yi-Fan Wang[1,2,*] Stephanie M. Brown[1,2,†] Lijing Shao[3,4,‡] and Wen Zhao[5,6,§]

[1]*Max-Planck-Institut für Gravitationsphysik (Albert-Einstein-Institut), D-30167 Hannover, Germany*
[2]*Leibniz Universität Hannover, D-30167 Hannover, Germany*
[3]*Kavli Institute for Astronomy and Astrophysics, Peking University, Beijing 100871, China*
[4]*National Astronomical Observatories, Chinese Academy of Sciences, Beijing 100012, China*
[5]*CAS Key Laboratory for Researches in Galaxies and Cosmology, Department of Astronomy,*
University of Science and Technology of China, Chinese Academy of Sciences, Hefei, Anhui 230026, China
[6]*School of Astronomy and Space Science, University of Science and Technology of China, Hefei 230026, China*

We report the results of testing gravitational-wave birefringence using the largest population of gravitational-wave events currently available. Gravitational-wave birefringence, which can arise from the effective field theory extension of general relativity, occurs when the parity symmetry is broken, causing the left- and right-handed polarizations to propagate following different equations of motion. We perform Bayesian inference on the 94 events reported by the 4th-Open Gravitational-wave Catalog (4-OGC) using a parity-violating waveform. We find no evidence for a violation of general relativity in the vast majority of events. However, the most massive event, GW190521, and the second most massive event, GW191109, show intriguing nonzero results for gravitational-wave birefringence. We find that the probability of association between GW190521 and the possible electromagnetic (EM) counterpart reported by Zwicky Transient Facility (ZTF) is increased when assuming birefringence. Excluding GW190521 and GW191109, the parity-violating energy scale is constrained to $M_{\rm PV} > 0.05$ GeV at 90% credible interval, which is an improvement over previous results from twelve events by a factor of five. We discuss the implications of our results on modified gravity and possible alternative explanations such as waveform systematics. More detections of massive binary black hole mergers from the upcoming LIGO/Virgo/KAGRA run will shed light on the true origin of the apparent birefringence.

I. INTRODUCTION

The advanced LIGO and Virgo [1,2] detectors have completed three observation runs (O1-O3) and announced the detection of ninety confident gravitational wave (GW) events in the Gravitational-Wave Transient Catalog (GWTC) [3–6]. Additional compact binary coalescence events are reported by independent analysis [7–12] of the public data [13]. The most recent version of Open Gravitational-wave Catalog, 4-OGC [11], used PyCBC toolkit [14] to search the public data from all three observation runs and reported ninety-four events [10]. 4-OGC agrees with GWTC for all

[*]yifan.wang@aei.mpg.de
[†]stephanie.brown@aei.mpg.de
[‡]lshao@pku.edu.cn
[§]wzhao7@ustc.edu.cn

confident events with a probability of astrophysical origin $p_{\rm astro} > 0.99$. The detection of GWs has enabled numerous precise tests of (GR) in the strong, dynamical field [15–21] and high energy (sub-GeV) regimes [22]. All the tests to date have confirmed that GW data is consistent with the predictions of GR.

This work tests GW birefringence using the currently largest population of gravitational-wave events from 4-OGC. Birefringence of GWs emerges when the parity symmetry, which is the invariance of physical laws regarding the inversion of spatial coordinates, is broken between the left- and right-handed GW polarizations. While parity symmetry is conserved in GR, theories where parity is violated have been proposed such as Chern-Simons gravity [23–27], Hořava-Lifshitz gravity [28–30], ghost-free scalar-tensor gravity [31], and the symmetric teleparallel equivalent of GR [32] to account for dark matter and dark energy. Parity violation also arises at high energy scales in quantum gravity theories such as loop quantum gravity and string theory [23].

We utilize an EFT extension of the linearized Einstein-Hilbert action to study how deviations from GR affect GW

propagation. EFT is a flexible framework that includes all action terms that purposely preserve or violate certain symmetries. The leading order higher derivative modification of the linearized action comes from terms of mass dimension five that violate parity [33,34]. Parity violation leads to an asymmetry in the propagation speeds and amplitudes of the left- and right-hand polarization of GW, which, in turn, leads to phase and amplitude birefringence, respectively. Given the relationship between parity violation and Lorentz violation [35], our tests have implications for constraining the standard model extension (SME) of gravity [36,37], which is the most general EFT extension of linearized GR that violates Lorentz symmetry.

Tests of GW birefringence were first done in ref. [38], where they checked for waveform peak splitting in the first-ever detected GW event, GW150914. Reference [39] constrained birefringence using the GW propagation speed measured from the binary neutron star merger event GW170817 [40], and Refs. [41–48] placed further constraints on birefringence using GWTC events.

We test for GW birefringence in ninety-four GW events and find no evidence of birefringence in ninety-two events. Intriguingly, we find two outliers, GW190521 and GW191109_010717 (hereafter GW191109), the most and second most massive binary black holes in 4-OGC [11,49,50], favor the birefringence waveform over the GR waveform with Bayes factors 11.0 and 22.9, respectively (ln $\mathcal{B}_{\mathrm{GR}}^{\mathrm{nonGR}} = 2.4$ and 3.1). Excluding these two outliers, we place constraints on the cutoff energy scale $M_{\mathrm{PV}} > 0.05$ GeV, which is more stringent than Ref. [22] by a factor of five due to the larger dataset and the more advanced waveform. The result can be mapped to the SME coefficient $|\vec{\zeta}^{(5)}| < 9 \times 10^{-16}$ m, which characterizes isotropic birefringence with mass dimension $d = 5$.

The nonzero results may be caused by non-Gaussian noise fluctuation, systematic errors in waveform templates, or physical effects that are outside the standard assumptions for quasicircular binary black hole mergers, e.g., the presence of orbital eccentricity [51,52], a hyperbolic encounter [53], or even entirely new physics [54]. We assess how the background noise affects the M_{pv} measurement for both GW190521 and GW191109 by injecting 100 GR signals into the detector noise around the observed coalescence time for each event. The results suggest that our detection of GR deviation for GW190521 and GW191109 is not likely an artifact of the noise.

Lastly, we consider the possible EM counterpart of GW190521, which ZTF observed and comes from an active galactic nucleus [55,56], by comparing the sky location posteriors for GW190521 with and without birefringence. Prior analyses of GW190521 do not strongly favor association with the EM counterpart. Reference [57] reported the Bayes factor of ln $B \gtrsim -4$ which disfavors a sky location fixed to that of the electromagnetic counterpart. However, if we assume GW birefringence, we find evidence in favor of the association with the EM counterpart with ln $\mathcal{B}$ of 6.6.

II. WAVEFORM TEMPLATES FOR GW BIREFRINGENCE

We briefly overview the construction of waveform templates to test GW birefringence following Ref. [34]. From the perspective of EFT, the leading order modifications to the linearized Einstein-Hilbert action are terms with three derivatives and mass dimension five: $\epsilon^{ijk}\dot{h}_{il}\partial_j\dot{h}_{kl}$ and $\epsilon^{ijk}\partial^2 h_{il}\partial_j h_{kl}$ [33,34,58], where $i, j\ldots = 1, 2, 3$ refer to spatial coordinates, ∂_j denotes spatial derivatives, dot denotes derivatives with respect to time, ∂^2 is the Laplacian, ϵ^{ijk} is the antisymmetric symbol, and h_{ij} is the tensor perturbation of metric. Notably, both terms violate parity. Therefore, EFT suggests that the leading order modification to GW propagation arises from parity-violation. We do not consider the more complicated anisotropic GW birefringence, for which the effects can be found in Refs. [38,48,59]. Combining the above higher derivative terms with the linearized Einstein-Hilbert action gives

$$S = \frac{1}{16\pi G} \int dt d^3 x a^3 \left[\frac{1}{4}\dot{h}_{ij}^2 - \frac{1}{4a^2}(\partial_k h_{ij})^2 + \frac{1}{4}\left(\frac{c_1}{a M_{\mathrm{PV}}}\epsilon^{ijk}\dot{h}_{il}\partial_j\dot{h}_{kl} + \frac{c_2}{a^3 M_{\mathrm{PV}}}\epsilon^{ijk}\partial^2 h_{il}\partial_j h_{kl}\right) \right], \quad (1)$$

where a is the cosmic scale factor, M_{PV} is the energy scale at which higher order modification starts to be relevant, and c_1 and c_2 are two undetermined functions of cosmic time; the speed of light and the reduced Planck's constant are set to $c = \hbar = 1$. Equation (1) is the generic form of the action; c_1, c_2, and M_{PV} can be mapped to the corresponding model parameters in a specific modified gravity theories [23–32], as explicitly demonstrated in Ref. [34].

The equation of motion for the GW circular polarization modes h_A, where $A = R$ or L for the right- and left-hand modes, is

$$h_A'' + (2 + \nu_A)\mathcal{H}h_A' + (1 + \mu_A)k^2 h_A = 0, \quad (2)$$

where $\mathcal{H}$ is the conformal Hubble parameter, k is the wave number, and a prime denotes the derivative with respect to the cosmic conformal time τ, μ_A, and ν_A are the phase and amplitude birefringence parameters. They have the exact forms

$$\nu_A = -[\rho_A c_1 k/(a M_{\mathrm{PV}})]'/\mathcal{H},$$
$$\mu_A = \rho_A(c_1 - c_2)k/(a M_{\mathrm{PV}}), \quad (3)$$

$\rho_A = \pm 1$ for left- and right-handed polarizations represents broken parity of GWs during propagation.

We focus on velocity birefringence because the modification to GW strain from amplitude birefringence is negligible [34]. The GR solution can be found by setting $\mu_A = \nu_A = 0$ in Eq. (2).

Solving Eq. (2) gives the left- and right-handed circular polarization modes with parity violation. They are related to the GR waveform by

$$h_L^{PV}(f) = h_L^{GR}(f)e^{-i\delta\Psi(f)}, \qquad h_R^{PV}(f) = h_R^{GR}(f)e^{i\delta\Psi(f)}. \quad (4)$$

The plus (h_+) and cross ($h_\times$) modes of GW are given by $h_+ = (h_L + h_R)/\sqrt{2}$ and $h_\times = (h_L - h_R)/(\sqrt{2}i)$.

For binary black holes, we use the IMRPhenomXPHM [60] GR waveform approximant, which includes subdominant harmonics and effects of precession; the IMRPhenomD_NRTidal [61–64] and IMRPhenomNSBH [65], waveforms, which account for tidal deformability, are used for binary neutron stars and neutron-star–black-hole mergers respectively.

The phase modification to the GR waveform takes the following form

$$\delta\Psi(f) = \frac{(\pi f)^2}{M_{PV}} \int_0^z \frac{(c_1 - c_2)(1 + z')dz'}{H_0\sqrt{\Omega_M(1 + z')^3 + \Omega_\Lambda}}, \quad (5)$$

where H_0 is the Hubble constant, z is the cosmic redshift, the frequency term f^2 corresponds to a modification at 5.5 post-Newtonian order, Ω_M is the matter density, and Ω_Λ is the dark energy density. We adopt a ΛCDM cosmology with parameters $\Omega_M = 0.3075$, $\Omega_\Lambda = 0.691$, and $H_0 = 67.8 \text{ km s}^{-1} \text{ Mpc}^{-1}$ [66] to convert luminosity distance to redshift for Eq. (5). As most GW detections are from the local Universe, we make the simplifying assumption that c_1, c_2 are constants and $c_1 - c_2$ is of order unity. This is done by attributing its order of magnitude to M_{PV}. Also note that we do not consider the special case where $c_1 = c_2$ exactly, and thus $\mu_A = 0$, in this work. This is the case for dynamical Chern-Simons gravity [67–69] and the constraints on amplitude birefringence in this case can be found in Refs. [41,45].

III. BAYESIAN INFERENCE

We use Bayesian parameter estimation and model selection to test GW birefringence. Given data $d(t)$, which is a sum of the detector noise $n(t)$ and a possible GW signal $h(t, \vec{\theta})$ characterized by parameters $\vec{\theta}$, Bayes theorem states that

$$P(\vec{\theta}|d, H) = \frac{P(d|\vec{\theta}, H)P(\vec{\theta}|H)}{P(d|H)}, \quad (6)$$

where $P(\vec{\theta}|d, H)$ is the posterior probability distribution for parameters $\vec{\theta}$, $P(\vec{\theta}|H)$ is the prior distribution containing

any *a priori* information, $P(d|\vec{\theta}, H)$ is the likelihood for obtaining the data given model parameters, $P(d|H)$ is a normalization factor called evidence, and H is the hypothesis for modeling the data. This work considers two competing hypotheses: $\mathcal{H}_{GR}$ where GWs are accurately described by GR and $\mathcal{H}_{nonGR}$ where GWs have birefringence and are described by Eq. (4). The Bayes factor, or the ratio of the evidences of two hypotheses,

$$\mathcal{B}_{GR}^{nonGR} = \frac{P(d|\mathcal{H}_{nonGR})}{P(d|\mathcal{H}_{GR})}, \quad (7)$$

quantifies the degree that data favor one hypothesis over another.

Using PyCBC INFERENCE [70], we numerically sample over all GW intrinsic (mass $m_{1,2}$, spin $\vec{s}_{1,2}$, and, in the case of neutron stars, tidal deformability $\Lambda_{1,2}$) and extrinsic parameters (luminosity distance d_L, inclination angle ι, polarization angle Ψ, right ascension α, declination δ, coalescence time t_c, and phase ϕ_c) as well as the parity violation parameter M_{PV}^{-1} for $\mathcal{H}_1$. The priors for the intrinsic and extrinsic parameters are the same as those in the 4-OGC [10] which are uniform for mass, spin amplitude, polarization, coalescence phase, and time. The distance prior is uniform in comoving volume. The spin orientation, sky location, and spatial orientation priors are isotropic. The prior for M_{PV}^{-1} is uniform in [0,200] GeV^{-1} except for the two outlier events which use [0,1000].

Assuming M_{PV}^{-1} is a universal quantity, the M_{PV}^{-1} posteriors from the individual GW events can be combined to obtain an overall constraint,

$$p(M_{PV}^{-1}|\{d_i\}, H_{nonGR}) \propto \prod_{i=1}^N p(M_{PV}^{-1}|d_i, H_{nonGR}), \quad (8)$$

where d_i denotes data of the ith GW event.

IV. RESULTS

We find that ninety-two out of ninety-four events are consistent with GR; the M_{PV}^{-1} posteriors are shown in Fig. 1, with the most constraining events individually indicated in the legend. In general, the tightest constraints are all from events with relatively low mass ($\sim 10\, M_\odot$) binary black hole mergers, e.g., GW190707_093326 has component masses of $12.9\, M_\odot$ and $7.7\, M_\odot$ [10]. This result is unsurprising because the birefringence effect is more significant at higher frequencies, where low mass binaries spend more time [see Eq. (5)].

The overall constraint is obtained by multiplying the posterior distributions of the individual events together using Eq. (8). We find the 90% upper limit of M_{PV}^{-1} to be 19 GeV^{-1}, which corresponds to $M_{PV} > 0.05$ GeV. This result is more stringent than previous results, based on twelve GW evens, by a factor of five [22]. Note that
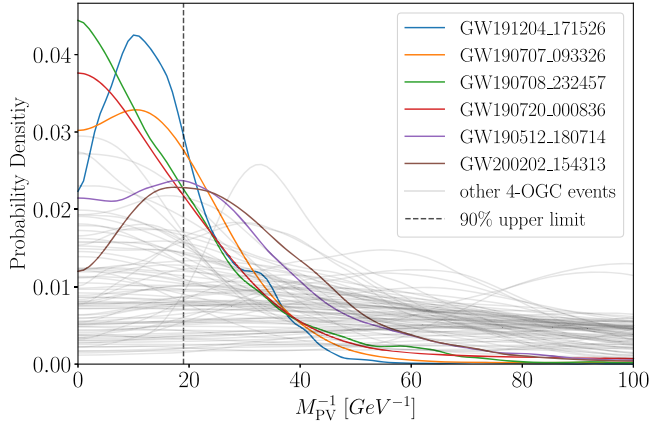
FIG. 1. The $M_{\rm PV}^{-1}$ posterior distributions for all 4-OGC events except GW190521 and GW191109. The legend indicates the events that give the tightest constraints. The vertical dashed line denotes the 90% upper limit for $M_{\rm PV}^{-1}$ from combined results.

Ref. [22] used $h = 1$ not $\hbar = 1$. Taking this into account, their result is $M_{\rm PV} > 0.01$ GeV. This improvement is due to the increased number of events analyzed and the use of improved GW waveforms [60] with longer duration and higher harmonic modes.

The limit on $M_{\rm PV}$ can be easily mapped to bounds on the SME coefficients that describe isotropic birefringence of GWs at mass dimension $d = 5$, via $|\vec{\varsigma}^{(5)}| \sim \frac{1}{4} M_{\rm PV}^{-1}$ [38,71]. For $M_{\rm PV} > 0.05$ GeV, one gets $|\vec{\varsigma}^{(5)}| < 9 \times 10^{-16}$ m, which is comparable to limits from Refs. [42,46].

A. GW190521 and GW191109

We find non-zero results for birefringence in GW190521 and GW191109 with $M_{\rm PV}^{-1} = 400_{-230}^{+460}$ GeV^{-1} and 220_{-100}^{+150} GeV^{-1} (90% credible interval). Furthermore, the Bayes factors support the non-GR hypothesis: $\mathcal{B}_{\rm GR}^{\rm nonGR} = 11.0$ and 22.9, respectively ($\ln \mathcal{B}_{\rm GR}^{\rm nonGR} = 2.4$ and 3.1). The $M_{\rm PV}^{-1}$, source frame chirp mass $\mathcal{M}^{src} = (m_1 m_2)^{3/5} / (m_1 + m_2)^{1/5}$, and mass ratio $q = m_1/m_2$, posteriors are shown in Fig. 2. $m_{1/2}$ are the heavier/lighter binary component masses. Intriguingly, GW190521 and GW191109 are the most and second most massive events found in 4-OGC.

To investigate any systematics causing the apparent deviation from GR, we perform two more birefringence tests for the outlier events using a different phenomenological template model IMRPhenomPv3HM [72] and a numerical relativity surrogate model NRSur7dq4 [73]. We find consistent support for nonzero $M_{\rm PV}^{-1}$ in the posteriors for these runs. We further check the data quality around GW190521 and GW191109 by calculating the background noise power spectral density (PSD) variation (see Ref. [74] for definition), which measures the noise nonstationarity. For GW190521, the PSD variation in a one-hour interval
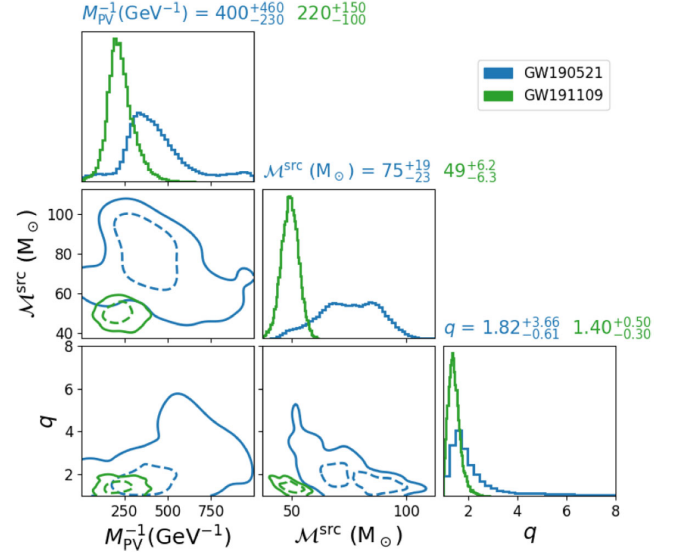

FIG. 2. Chirp mass, mass ratio, and $M_{\rm PV}^{-1}$ posterior distributions for GW190521 and GW191109. The dashed (solid) two-dimensional contours denote the 50% (90%) credible intervals. The diagonal plots are the one-dimensional marginalization for the posterior.

around the event only deviates from Gaussian stationary noise by $\lesssim 0.1$ (except for a glitch in LIGO Hanford 400 s after the event), showing no significant deviation from other ordinary times. However, the LIGO detector data for GW191109 contains non-Gaussian and nonstationary transient noise artifacts or glitches [6]. Due to this, we performed our analysis using data with the glitch removed released by LIGO/Virgo [6].

To further quantify whether detector noise could be the cause of the observed nonzero result, we simulate 100 GR signals with parameters drawn from the GW190521 and GW191109 posteriors [11] and inject them into the LIGO/Virgo detector noise nearby the GW190521 and GW191109 triggers, respectively (see the Appendix for technical details). We find only 1(4) events, out of 100 injections, have $\ln B_{\rm GR}^{\rm nonGR}$ larger than what we found for GW190521(GW191109). We thus conclude that the false alarm rate for detecting birefringence is 1(4) in 100 observations.

Lastly, we consider the possible EM counterpart for GW190521 reported by the ZTF [55,56]. Interestingly, we find that including birefringence significantly improves the chance of association. Figure 3 shows the right ascension (α), declination (δ), and luminosity distance posteriors from the birefringence analysis. The red lines mark the independent measurements by ZTF ($\alpha = 3.36$ rad, $\delta = 0.61$ rad, and redshift $= 0.438$). The Bayes factor supports coincidence with $\ln \mathcal{B}_{\rm overlap} = 6.6$ in favor of the association. The GR analyses did not favor association. For instance, Ref. [57] reports $\ln \mathcal{B}_{\rm overlap} \sim -4.4$.
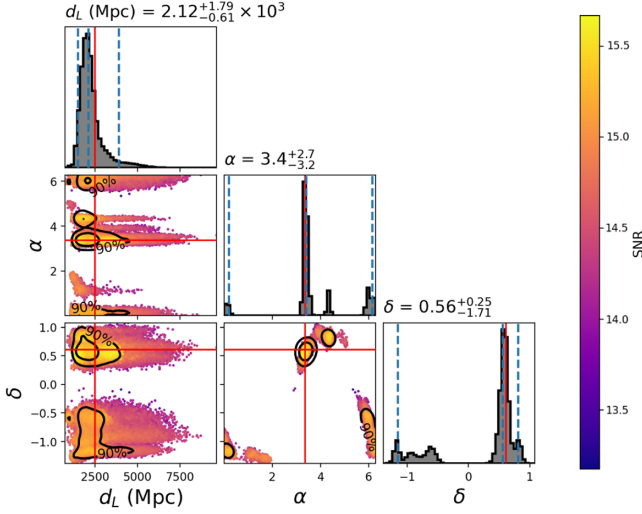
FIG. 3. Posterior distributions for luminosity distance d_L, right ascension α, and declination δ for GW190521 assuming birefringence. The median values and 90% credible interval are denoted with dotted vertical lines; the vertical color bar shows the signal-to-noise ratio. The red lines mark the sky location of a possible EM flare associated with GW190521.

V. DISCUSSION AND CONCLUSION

We test for GW propagation birefringence using state-of-the-art waveform templates and 4-OGC, the most extensive GW catalog currently available. Combining the results from all of the events except the outliers GW190521 and GW191109, we constrain the lower energy scale cutoff to $M_{PV} > 0.05$ GeV, which is an improvement over previous constraints by a factor of 5. The constraint on M_{PV} allows us to limit the SME isotropic birefringence parameter with mass dimension $d = 5$ to $|\vec{\zeta}^{(5)}| < 9 \times 10^{-16}$ m. These results show that GW astronomy is a promising future avenue by which to study gravity at high energies.

We surprisingly find evidence in support of GW birefringence for GW190521 and GW191109, which happen to be the most and second most massive events in 4-OGC. Furthermore, we find that including birefringences increases the likelihood of association between GW190521 and its possible EM counterpart.

We find no disparity between three state-of-the-art waveform approximants and no significant issues with the data quality for GW190521. While there is a glitch in the GW191109 data, it was removed by LIGO/Virgo, and our analysis suggests the noise fluctuation is unlikely to have caused the non-zero M_{PV}^{-1} result.

However, it is well documented that GW190521 is an exceptional event that may not fit well into the simple quasicircular binary black hole merger picture. For instance, Refs. [51,52] show that GW190521 is consistent with the merger of a binary black hole system with eccentric orbit, Ref. [53] gives a Bayes factor that highly favors a hyperbolic encounter over a quasicircular merger,

and Ref. [54] shows that GW190521 could be genuinely new physics, such as a Proca star collision. The accuracy of current GR waveform approximants is limited at the merger stage. This is quite relevant for GW190521 and GW110919 as most of the data is in the merger band. Our work provides further evidence for nonstandard physical effects in GW data, which the available GR waveform approximants cannot currently account for. Even if the apparent deviation from GR is from new physics, our GW birefringence model cannot provide a universal explanation. A possible extension might include a parity violation that depends on the masses of the binary.

As the advanced LIGO and Virgo detectors are upgraded and the KAGRA detector joins the network, we expect more high mass detections similar to GW190521 and GW191109, which may provide further insight into the physics behind the observed behavior of these outliers.

We release all posterior files and the scripts necessary to reproduce this work in [75].

APPENDIX: INVESTIGATION ON DATA QUALITY SYSTEMATICS BY GR INJECTION

We investigate the data quality to determine if nonstationary or non-Gaussian noise could be responsible for the apparent deviation from GR for GW190521 and GW191109. We generate 100 GR waveforms with the IMRPhenomXPHM [60] template and inject them into the LIGO and Virgo data near the coalescence times of GW190521 and GW191109. The waveform source parameters (component masses and spins, sky location, source orbital orientation, GW polarization angle, and coalescence phase) are sampled from the GW190521 and GW191109 posteriors released by 4-OGC [11]. For GW190521, the
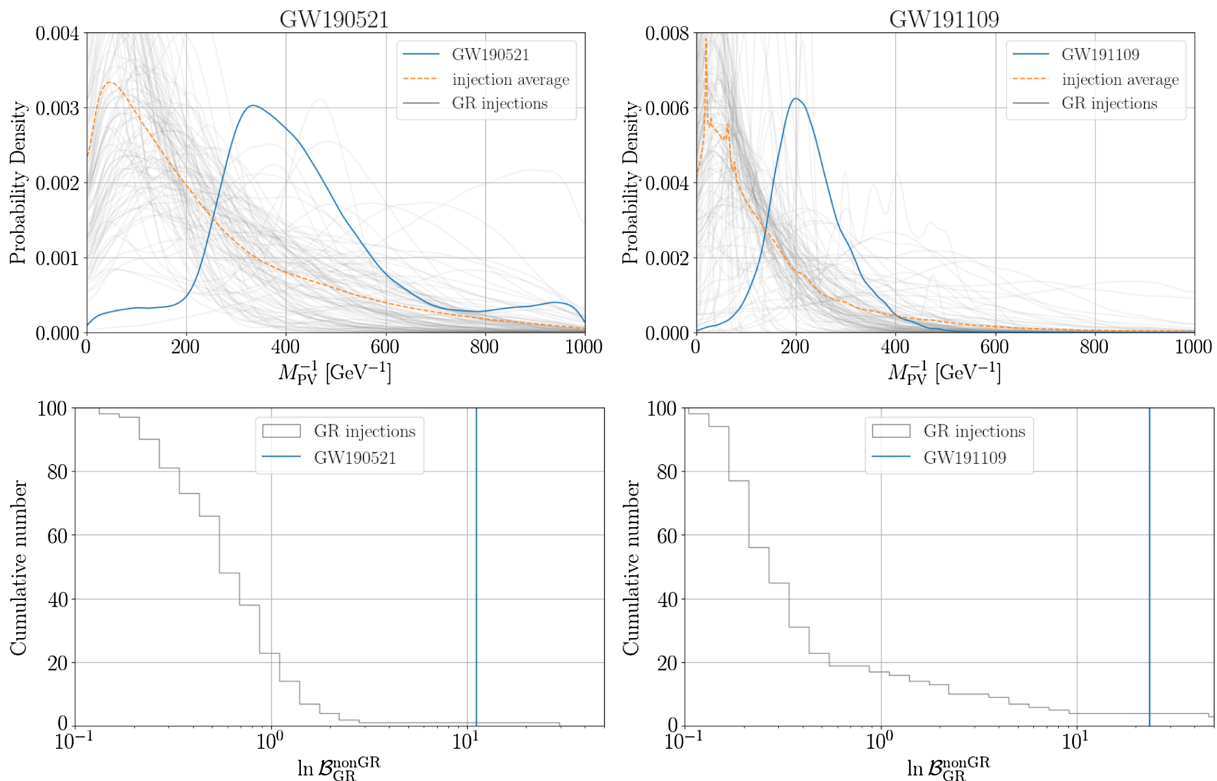
FIG. 4.　First row: the Bayesian posteriors of M_{PV}^{-1} for 100 GR injections that mimic GW190521 (left) and GW191109 (right). The posteriors for GW191109 and GW1905121 are plotted for comparison. The average posterior of the 100 injections is shown. Second row: the cumulative distribution of $\ln \mathcal{B}_{\mathrm{GR}}^{\mathrm{nonGR}}$ for GR injections. The histogram shows the number of injections with $\ln \mathcal{B}_{\mathrm{GR}}^{\mathrm{nonGR}}$ equal or less than certain values. The Bayes factor for the real events is plotted as a comparison.

waveforms are injected into the time interval $[-20, 20]$ seconds around the trigger time of GW190521. However, we exclude the region $[-4, 4]$ seconds around the trigger time, where the event is predominant over the noise. Both LIGO detectors contain transient noise artifacts at the merger time of GW191109 [6]. We have analyzed GW191109 using a deglitched version of data released by LIGO and Virgo [6]. However, a cleaned version of the data in the region of GW191109 is not readily available. To avoid the glitches, which were removed for the GW191109 analysis, we inject our signals into a segment of data $[-100, -30]$ seconds from the trigger.

The injections are then analyzed the same as the actual event using the method presented in the main text. For the parameter estimation, all priors are the same as those used to analyze the GW190911 and GW190521, respectively.

The injections' M_{PV}^{-1} posteriors are shown in the first row of Fig. 4. For comparison, the figure also shows the GW190521 and GW191109 posteriors. We note that some results for GW191109-type injections have a spikey or

multimodal shape; we attribute this to the noisy data around GW191109.

We find that, in rare cases, the background noise fluctuation can produce nonzero peaks for M_{PV}^{-1}. To assess the significance of our non-zero M_{PV}^{-1} results for GW191109 and GW190521, we extract the Bayes factor from the posteriors using the Savage-Dickey density ratio; the second row of Fig. 4 shows the results. Using $\ln B_{\mathrm{GR}}^{\mathrm{nonGR}}$ as a statistic, only 1 in 100 and 4 in 100 simulations exceed the Bayes factor from GW190521 and GW191109, respectively. The false alarm rate or p-value to reject the null hypothesis that GR is correct is thus 1(4) out of 100 realizations.

We take the mean of M_{PV}^{-1} of all injections to determine the background distribution for the null hypothesis and note that the background is qualitatively different from the actual data results. Overall we do not find strong evidence that background noise artifacts caused the nonzero results for testing GR.

[1] J. Aasi *et al.* (LIGO Scientific Collaboration), Advanced LIGO, Classical Quantum Gravity **32,** 074001 (2015).

[2] F. Acernese *et al.* (VIRGO Collaboration), Advanced Virgo: A second-generation interferometric gravitational wave detector, Classical Quantum Gravity **32,** 024001 (2015).

[3] B. P. Abbott *et al.* (LIGO Scientific and Virgo Collaborations), GWTC-1: A Gravitational-Wave Transient Catalog of Compact Binary Mergers Observed by LIGO and Virgo during the First and Second Observing Runs, Phys. Rev. X **9,** 031040 (2019).

[4] R. Abbott *et al.* (LIGO Scientific and Virgo Collaborations), GWTC-2: Compact Binary Coalescences Observed by LIGO and Virgo During the First Half of the Third Observing Run, Phys. Rev. X **11,** 021053 (2021).

[5] R. Abbott *et al.* (LIGO Scientific and Virgo Collaboration), Gwtc-2.1: Deep extended catalog of compact binary coalescences observed by LIGO and Virgo during the first half of the third observing run, arXiv:2108.01045.

[6] R. Abbott *et al.* (LIGO Scientific, VIRGO, and KAGRA Collaborations), GWTC-3: Compact binary coalescences observed by LIGO and Virgo during the second part of the third observing run, arXiv:2111.03606.

[7] Alexander H. Nitz, Collin Capano, Alex B. Nielsen, Steven Reyes, Rebecca White, Duncan A. Brown, and Badri Krishnan, 1-OGC: The first open gravitational-wave catalog of binary mergers from analysis of public Advanced LIGO data, Astrophys. J. **872,** 195 (2019).

[8] Alexander H. Nitz, Thomas Dent, Gareth S. Davies, Sumit Kumar, Collin D. Capano, Ian Harry, Simone Mozzon, Laura Nuttall, Andrew Lundgren, and Márton Tápai, 2-OGC: Open gravitational-wave catalog of binary mergers from analysis of public Advanced LIGO and Virgo data, Astrophys. J. **891,** 123 (2019).

[9] Tejaswi Venumadhav, Barak Zackay, Javier Roulet, Liang Dai, and Matias Zaldarriaga, New binary black hole mergers in the second observing run of Advanced LIGO and Advanced Virgo, Phys. Rev. D **101,** 083030 (2020).

[10] Alexander H. Nitz, Collin D. Capano, Sumit Kumar, Yi-Fan Wang, Shilpa Kastha, Marlin Schäfer, Rahul Dhurkunde, and Miriam Cabero, 3-OGC: Catalog of gravitational waves from compact-binary mergers, Astrophys. J. **922,** 76 (2021).

[11] Alexander H. Nitz, Sumit Kumar, Yi-Fan Wang, Shilpa Kastha, Shichao Wu, Marlin Schäfer, Rahul Dhurkunde, and Collin D. Capano, 4-OGC: Catalog of gravitational waves from compact-binary mergers, arXiv:2112.06878.

[12] Seth Olsen, Tejaswi Venumadhav, Jonathan Mushkin, Javier Roulet, Barak Zackay, and Matias Zaldarriaga, New binary black hole mergers in the LIGO–Virgo O3a data, Phys. Rev. D **106,** 043009 (2022).

[13] B. P. Abbott *et al.*, Open data from the first and second observing runs of Advanced LIGO and Advanced Virgo, SoftwareX **13,** 100658 (2021).

[14] Alexander H. Nitz, Ian W. Harry, Joshua L. Willis, Christopher M. Biwer, Duncan A. Brown, Larne P. Pekowsky, T. Dal Canton, Andrew R. Williamson, Thomas Dent, Collin D. Capano, Thomas J. Massinger, Amber K. Lenon, Alex B. Nielsen, and Miriam Cabero, PyCBC Software, https://github.com/gwastro/pycbc (2018).

[15] R. Abbott *et al.* (LIGO Scientific and Virgo Collaborations), Tests of general relativity with binary black holes from the second LIGO-Virgo gravitational-wave transient catalog, Phys. Rev. D **103,** 122002 (2021).

[16] B. P. Abbott *et al.* (LIGO Scientific and Virgo Collaboration), Tests of general relativity with the binary black hole signals from the LIGO-Virgo catalog GWTC-1, Phys. Rev. D **100,** 104036 (2019).

[17] B. P. Abbott *et al.* (Virgo and LIGO Scientific Collaboration), Tests of General Relativity with GW150914, Phys. Rev. Lett. **116,** 221101 (2016); Erratum, Phys. Rev. Lett. **121,** 129902 (2018).

[18] Katerina Chatziioannou, Maximiliano Isi, Carl-Johan Haster, and Tyson B. Littenberg, Morphology-independent test of the mixed polarization content of transient gravitational wave signals, Phys. Rev. D **104,** 044005 (2021).

[19] Remya Nair, Scott Perkins, Hector O. Silva, and Nicolás Yunes, Fundamental Physics Implications for Higher-Curvature Theories from Binary Black Hole Signals in the LIGO-Virgo Catalog GWTC-1, Phys. Rev. Lett. **123,** 191101 (2019).

[20] R. Abbott, H. Abe, F. Acernese, K. Ackley *et al.*, Tests of general relativity with GWTC-3, arXiv:2112.06861 [Phys. Rev. D (to be published)].

[21] Ajit Kumar Mehta, Alessandra Buonanno, Roberto Cotesta, Abhirup Ghosh, Noah Sennett, and Jan Steinhoff, Tests of general relativity with gravitational-wave observations using a flexible–theory-independent method, arXiv:2203.13937.

[22] Yi-Fan Wang, Rui Niu, Tao Zhu, and Wen Zhao, Gravitational wave implications for the parity symmetry of gravity in the high energy region, Astrophys. J. **908,** 58 (2021).

[23] Nicolas Yunes, K. G. Arun, Emanuele Berti, and Clifford M. Will, Post-circular expansion of eccentric binary inspirals: Fourier-domain waveforms in the stationary phase approximation, Phys. Rev. D **80,** 084001 (2009); Erratum, Phys. Rev. D **89,** 109901 (2014).

[24] Daiske Yoshida and Jiro Soda, Exploring the string axiverse and parity violation in gravity with gravitational waves, Int. J. Mod. Phys. D **27,** 1850096 (2018).

[25] Chong-Sun Chu, Jiro Soda, and Daiske Yoshida, Gravitational waves in axion dark matter, Universe **6,** 89 (2020).

[26] Sunghoon Jung, Taehun Kim, Jiro Soda, and Yuko Urakawa, Constraining the gravitational coupling of axion dark matter at LIGO, Phys. Rev. D **102,** 055013 (2020).

[27] Kohei Kamada, Jun'ya Kume, and Yusuke Yamada, Chiral gravitational effect in time-dependent backgrounds, J. High Energy Phys. 05 (2021) 292.

[28] Petr Hořava, Quantum gravity at a Lifshitz point, Phys. Rev. D **79,** 084008 (2009).

[29] Anzhong Wang, Qiang Wu, Wen Zhao, and Tao Zhu, Polarizing primordial gravitational waves by parity violation, Phys. Rev. D **87,** 103512 (2013).

[30] Tomohiro Takahashi and Jiro Soda, Chiral Primordial Gravitational Waves from a Lifshitz Point, Phys. Rev. Lett. **102,** 231301 (2009).

[31] M. Crisostomi, K. Noui, C. Charmousis, and D. Langlois, Beyond Lovelock gravity: Higher derivative metric theories, Phys. Rev. D **97,** 044034 (2018).

[32] Aindriú Conroy and Tomi Koivisto, Parity-violating gravity and GW170817 in non-Riemannian cosmology, J. Cosmol. Astropart. Phys. 12 (2019) 016.

[33] Paolo Creminelli, Jérôme Gleyzes, Jorge Noreña, and Filippo Vernizzi, Resilience of the Standard Predictions for Primordial Tensor Modes, Phys. Rev. Lett. **113,** 231301 (2014).

[34] Wen Zhao, Tao Zhu, Jin Qiao, and Anzhong Wang, Waveform of gravitational waves in the general parity-violating gravities, Phys. Rev. D **101,** 024002 (2020).

[35] O. W. Greenberg, *CPT* Violation Implies Violation of Lorentz Invariance, Phys. Rev. Lett. **89,** 231602 (2002).

[36] V.Alan Kostelecky, Gravity, Lorentz violation, and the standard model, Phys. Rev. D **69,** 105009 (2004).

[37] Jay D. Tasson, The standard-model extension and gravitational tests, Symmetry **8,** 111 (2016).

[38] V. Alan Kostelecký and Matthew Mewes, Testing local Lorentz invariance with gravitational waves, Phys. Lett. B **757,** 510 (2016).

[39] Atsushi Nishizawa and Tsutomu Kobayashi, Parity-violating gravity and GW170817, Phys. Rev. D **98,** 124018 (2018).

[40] B. P. Abbott *et al.* (LIGO Scientific and Virgo Collaborations), GW170817: Observation of Gravitational Waves from a Binary Neutron Star Inspiral, Phys. Rev. Lett. **119,** 161101 (2017).

[41] Remya Nair, Scott Perkins, Hector O. Silva, and Nicolás Yunes, Fundamental Physics Implications for Higher-Curvature Theories from Binary Black Hole Signals in the LIGO-Virgo Catalog GWTC-1, Phys. Rev. Lett. **123,** 191101 (2019).

[42] Lijing Shao, Combined search for anisotropic birefringence in the gravitational-wave transient catalog GWTC-1, Phys. Rev. D **101,** 104019 (2020).

[43] Sai Wang and Zhi-Chao Zhao, Tests of *CPT* invariance in gravitational waves with LIGO-Virgo catalog GWTC-1, Eur. Phys. J. C **80,** 1032 (2020).

[44] Kei Yamada and Takahiro Tanaka, Parametrized test of parity-violating gravity using GWTC-1 events, Prog. Theor. Exp. Phys. **2020,** 093E01 (2020).

[45] Maria Okounkova, Will M. Farr, Maximiliano Isi, and Leo C. Stein, Constraining gravitational wave amplitude birefringence and Chern-Simons gravity with GWTC-2, Phys. Rev. D **106,** 044067 (2022).

[46] Ziming Wang, Lijing Shao, and Chang Liu, New limits on the Lorentz/CPT symmetry through fifty gravitational-wave events, Astrophys. J. **921,** 158 (2021).

[47] Zhi-Chao Zhao, Zhoujian Cao, and Sai Wang, Search for the birefringence of gravitational waves with the third observing run of Advanced LIGO-Virgo, Astrophys. J. **930,** 139 (2022).

[48] Rui Niu, Tao Zhu, and Wen Zhao, Constraining anisotropy birefringence dispersion in gravitational wave propagation with GWTC-3, arXiv:2202.05092.

[49] R. Abbott *et al.* (LIGO Scientific and Virgo Collaborations), GW190521: A Binary Black Hole Merger with a Total Mass of 150 $M_\odot$, Phys. Rev. Lett. **125,** 101102 (2020).

[50] R. Abbott *et al.* (LIGO Scientific and Virgo Collaborations), Properties and astrophysical implications of the 150 $M_\odot$ binary black hole merger GW190521, Astrophys. J. Lett. **900,** L13 (2020).

[51] Isobel M. Romero-Shaw, Paul D. Lasky, Eric Thrane, and Juan Calderon Bustillo, GW190521: Orbital eccentricity and signatures of dynamical formation in a binary black hole merger signal, Astrophys. J. Lett. **903,** L5 (2020).

[52] V. Gayathri, J. Healy, J. Lange, B. O'Brien, M. Szczepanczyk, I. Bartos, M. Campanelli, S. Klimenko, C. Lousto, and R. O'Shaughnessy, GW190521 as a highly eccentric black hole merger, Nat. Astron. **6,** 344 (2022).

[53] Rossella Gamba, Matteo Breschi, Gregorio Carullo, Piero Rettegno, Simone Albanesi, Sebastiano Bernuzzi, and Alessandro Nagar, GW190521: A dynamical capture of two black holes, arXiv:2106.05575.

[54] Juan Calderón Bustillo, Nicolas Sanchis-Gual, Alejandro Torres-Forné, José A. Font, Avi Vajpeyi, Rory Smith, Carlos Herdeiro, Eugen Radu, and Samson H. W. Leong, Gw190521 as a Merger of Proca Stars: A Potential New Vector Boson of 8.7×10^{-13} eV, Phys. Rev. Lett. **126,** 081101 (2021).

[55] M. J. Graham *et al.*, Candidate Electromagnetic Counterpart to the Binary Black Hole Merger Gravitational Wave Event S190521g, Phys. Rev. Lett. **124,** 251102 (2020).

[56] Gregory Ashton, Kendall Ackley, Ignacio Magaña Hernandez, and Brandon Piotrzkowski, Current observations are insufficient to confidently associate the binary black hole merger GW190521 with AGN J124942.3 + 344929, Classical Quantum Gravity **38,** 235004 (2021).

[57] Alexander H. Nitz and Collin D. Capano, GW190521 may be an intermediate-mass ratio inspiral, Astrophys. J. **907,** L9 (2021).

[58] Xian Gao and Xun-Yang Hong, Propagation of gravitational waves in a cosmological background, Phys. Rev. D **101,** 064057 (2020).

[59] Kellie O'Neal-Ault, Quentin G. Bailey, Tyann Dumerchat, Leila Haegel, and Jay Tasson, Analysis of birefringence and dispersion effects from spacetime-symmetry breaking in gravitational waves, Universe **7,** 380 (2021).

[60] Geraint Pratten *et al.*, Computationally efficient models for the dominant and subdominant harmonic modes of precessing binary black holes, Phys. Rev. D **103,** 104056 (2021).

[61] Sebastian Khan, Sascha Husa, Mark Hannam, Frank Ohme, Michael Pürrer, Xisco Jiménez Forteza, and Alejandro Bohé, Frequency-domain gravitational waves from non-precessing black-hole binaries. ii. a phenomenological model for the advanced detector era, Phys. Rev. D **93,** 044007 (2016).

[62] Sascha Husa, Sebastian Khan, Mark Hannam, Michael Pürrer, Frank Ohme, Xisco Jiménez Forteza, and Alejandro Bohé, Frequency-domain gravitational waves from nonprecessing black-hole binaries. I. New numerical waveforms and anatomy of the signal, Phys. Rev. D **93,** 044006 (2016).

[63] Tim Dietrich, Sebastiano Bernuzzi, and Wolfgang Tichy, Closed-form tidal approximants for binary neutron star gravitational waveforms constructed from high-resolution numerical relativity simulations, Phys. Rev. D **96,** 121501 (2017).

[64] Tim Dietrich *et al.*, Matter imprints in waveform models for neutron star binaries: Tidal and self-spin effects, Phys. Rev. D **99,** 024029 (2019).

[65] Jonathan E. Thompson, Edward Fauchon-Jones, Sebastian Khan, Elisa Nitoglia, Francesco Pannarale, Tim Dietrich, and Mark Hannam, Modeling the gravitational wave

signature of neutron star black hole coalescences, Phys. Rev. D **101,** 124059 (2020).

[66] P. A. R. Ade *et al.* (Planck Collaboration), Planck 2015 results. XIII. Cosmological parameters, Astron. Astrophys. **594,** A13 (2016).

[67] Nicolas Yunes, Richard O'Shaughnessy, Benjamin J. Owen, and Stephon Alexander, Testing gravitational parity violation with coincident gravitational waves and short gamma-ray bursts, Phys. Rev. D **82,** 064017 (2010).

[68] Kent Yagi and Huan Yang, Probing gravitational parity violation with gravitational waves from stellar-mass black hole binaries, Phys. Rev. D **97,** 104018 (2018).

[69] Stephon H. Alexander and Nicolás Yunes, Gravitational wave probes of parity violation in compact binary coalescences, Phys. Rev. D **97,** 064033 (2018).

[70] C. M. Biwer, Collin D. Capano, Soumi De, Miriam Cabero, Duncan A. Brown, Alexander H. Nitz, and V. Raymond, PyCBC inference: A python-based parameter estimation toolkit for compact binary coalescence signals, Publ. Astron. Soc. Pac. **131,** 024503 (2019).

[71] Matthew Mewes, Signals for Lorentz violation in gravitational waves, Phys. Rev. D **99,** 104062 (2019).

[72] Sebastian Khan, Frank Ohme, Katerina Chatziioannou, and Mark Hannam, Including higher order multipoles in gravitational-wave models for precessing binary black holes, Phys. Rev. D **101,** 024056 (2020).

[73] Vijay Varma, Scott E. Field, Mark A. Scheel, Jonathan Blackman, Davide Gerosa, Leo C. Stein, Lawrence E. Kidder, and Harald P. Pfeiffer, Surrogate models for precessing binary black hole simulations with unequal masses, Phys. Rev. Res. **1,** 033015 (2019).

[74] S. Mozzon, L. K. Nuttall, A. Lundgren, T. Dent, S. Kumar, and A. H. Nitz, Dynamic normalization for compact binary coalescence searches in non-stationary noise, Classical Quantum Gravity **37,** 215014 (2020).

[75] Y.-F. Wang *et al.*, Data release for "Tests of gravitational-wave birefringence with the open gravitational-wave catalog" (2022), https://github.com/gwastro/4ogc-birefringence.

[76] https://www.gw-openscience.org.